Mon. Not. R. Astron. Soc. **361,** 1393–1398 (2005) doi:10.1111/j.1365-2966.2005.09272.x

X-ray spectral evolution of Her X-1 in a low state and the following short high state

Sıtkı Cağdaş İnam[1⋆] and Altan Baykal[2⋆]

[1]*Department of Electrical and Electronics Engineering, Başkent University, Ankara 06530, Turkey*
[2]*Physics Department, Middle East Technical University, Ankara 06531, Turkey*

Accepted 2005 June 6. Received 2005 June 3; in original form 2005 April 26

ABSTRACT

We analysed spectral variations of ∼8.5-d long *Rossi X-ray Timing Explorer* (*RXTE*) monitoring observations of Her X-1 in 2001 December. This set of observations enables, for the first time, frequent continuous monitoring (111 pointings in ∼8.5 d) of the source with *RXTE* including a ∼1.7-d-long low state part and the following ∼6.8-d-long short high state part. We used an absorbed power-law model with an iron line energy complex modelled as a Gaussian to fit both the 3–60 keV Proportional Counter Array–High Energy X-ray Timing Experiment (PCA–HEXTE) overall short high state spectrum and 3–20 keV individual PCA spectra. An additional partial cold absorber model was used for both cases. Using 3–20 keV individual PCA spectra, absorption in anomalous dips (ADs) and pre-eclipse dips (PDs) in the short high state was compared. Decreasing the ratio of unabsorbed to absorbed flux with increasing unabsorbed flux in ADs and PDs was interpreted as evidence of the fact that the regions causing opaque obscuration and soft absorption are not geometrically far away from each other. Higher iron line peak energies in the low state and the short high state (∼6.6–6.9 keV) were interpreted as a clue of the presence of iron line components other than the Kα emission line.

Key words: stars: neutron – stars: pulsars: individual: Her X-1 – X-rays: binaries – X-rays: stars.

1 INTRODUCTION

Her X-1, being an eclipsing accretion powered pulsar consisting of a ∼1.24-s period pulsar in a ∼1.7-d circular orbit, was discovered in 1972 during *Uhuru* observations (Tananbaum et al. 1972). Soon after its discovery, its optical companion was identified to be the blue variable 13th-magnitude star HZ Her (Davidsen et al. 1972). The Her X-1/Hz Her binary system was shown to display a 35-d-long cycle of high and low X-ray flux states. There are two high states, main high and short high, within a single 35-d cycle lasting roughly about 10 and 5 d, respectively, and separated by ∼10-d-long low states (Giacconi et al. 1973; Scott & Leahy 1999). Superposed on this cycle are eclipses of the neutron star by the companion once per orbital period. While the 35-d cycle is mostly coherent since the discovery of the source, there have been four occasions so far when the high states have either failed to turn on or the main high state flux has been reduced (i.e. *anomalous low states*, see Parmar et al. 1985; Vrtilek et al. 1994; Oosterbroek et al. 2000; Boyd, Still & Corbet 2004).

The nature of the 35-d cycle is generally attributed to the periodic variable obscuration of the emission region by a precessing accretion disc viewed nearly edge-on (e.g. Petterson 1975; Scott & Leahy 1999; Scott, Leahy & Wilson 2000; Leahy 2004). It has been claimed that there is no strict periodicity of this precession (Ogelman 1987): '35-d cycles' generally have durations of 20, 20.5 and 21 orbital cycles with equal statistical probabilities, which may lead to the idea that the precession and orbital cycles are related physically (Scott & Leahy 1999). Baykal et al. (1993) revealed that the statistical interpretation of turn-on behaviour is consistent with a white-noise process in the first derivative of the 35-d phase fluctuations. Other manifestations of 35-d cycle include spectral variations in 35 d (Mihara 1991; Choi et al. 1994b; Zane et al. 2004; Leahy 1995, 2001), 35-d X-ray pulse profile evolution (Scott et al. 2000), optical pulsations occurring at certain 35 d and orbital phases (Middleditch 1983), and systematic 35-d variations in the optical light curve (Deeter et al. 1976; Gerend & Boynton 1976).

Distinct features of high states of Her X-1 in X-ray band are the pre-eclipse X-ray absorption dips occurring at ∼0.8 orbital phase (Giacconi et al. 1973; Crosa & Boynton 1980), and ADs (Giacconi et al. 1973; Scott & Leahy 1999) occurring at ∼0.4 orbital phase. Both types of dips are thought to be due to absorption of cold matter on the line of sight. The occurrence period of the X-ray dips is thought to be related to the beat period of 35 d and 1.7 d (∼1.65 d); thus they progress to earlier orbital phases within main high and short high states. More detailed features of the pre-eclipse and ADs of Her X-1 were discussed by Leahy, Yoshida & Matsuoka (1994),

⋆E-mail: inam@baskent.edu.tr (SCI); altan@astroa.physics.metu.edu.tr (AB)

© 2005 RAS

Downloaded from https://academic.oup.com/mnras/article-abstract/361/4/1393/1119646 by MIDDLE EAST TECHNICAL UNIVERSITY LIBRARY user on 23 July 2020

Reynolds & Parmar (1995), Leahy (1997), Shakura et al. (1998) and Stelzer et al. (1999).

Although considerable changes in the X-ray spectrum in 35-d cycle have been found to be evident, the X-ray spectrum in different 35-d phases can be fitted using a constant-emission model with varying absorption (e.g. Mihara et al. 1991; Leahy 2001). This is another property supporting the fact that 35-d cycle is due to the precession of an accretion disc that periodically obscures the neutron star beam. In other words, spectral variations in the X-ray band are not primarily due to the variations of the primary outgoing beam of the neutron star but rather due to changes in absorption.

Being the first accretion-powered pulsar found to have cyclotron absorption features (Truemper et al. 1978), the X-ray spectrum of Her X-1 shows this absorption feature around ∼40 keV, which indicates a surface magnetic field of $\sim(3.5–4.5) \times 10^{12}$ G. There is no evidence of a second harmonic around ∼80 keV (Coburn et al. 2002).

An iron line complex at ∼6.5 keV is evident in the X-ray spectrum of Her X-1 (Leahy 2001 and references therein). Furthermore, Endo, Nagase & Mihara (2000) were able to resolve the feature into two discrete emission lines at ∼6.4 and ∼6.7 keV. A distinct Fe XXVI line at ∼7 keV was detected with *XMM–Newton* throughout 35-d cycle except the main high (Zane et al. 2004). Variations in the iron line complex feature over the 35-d period and the spin period have been evident (e.g. Choi et al. 1994b), while variations of this complex feature with the orbital phase have also been studied (e.g. Zane et al. 2004).

In this paper, results of spectral analysis of the 2001 December low state and short high state *Rossi X-ray Timing Explorer* (*RXTE*) data of Her X-1 are presented. This set of observations enables, for the first time, frequent continuous monitoring (111 pointings in ∼8.5 d) of the source with *RXTE* including ∼1.7-d (≃1 orbital period) low state part and the following ∼6.8-d (≃4 orbital periods) short high state part. Section 2 is an overview about the instruments and the observations. In Section 3, we present the analysis of the observations. In Section 4, results are discussed.

2 INSTRUMENTS AND OBSERVATIONS

The *RXTE* observations used in this paper cover the period from 2001 December 18 to 26 (MJD 52261-52269) with a total exposure of 281.2 ks (Fig. 1). These observations have the common proposal ID 60017. The results presented here are based on data collected with the Proportional Counter Array (PCA, Jahoda et al. 1996) and the High Energy X-ray Timing Experiment (HEXTE; Rothschild et al. 1998). The PCA instrument consists of an array of five proportional counter units (PCUs) operating in the 2–60 keV energy range, with a total effective area of approximately 6250 cm^2 and a field of view of ∼1° FWHM (full width at half-maximum). Although the number of active PCUs varied between two and five during the observations, observations after 2000 May 13 belong to the observational epoch for which the background level for one of the PCUs it (PCU0) increased due to the fact that it started to operate without a propane layer. The latest combined background models are used together with FTOOLS 5.3 to estimate the appropriate PCA background. The HEXTE instrument consists of two independent clusters of detectors, each cluster containing four Na I(Tl)/CsI(Na) PHOSWICH scintillation counters (one of the detectors in cluster 2 is not used for spectral information) sharing a common ∼1° FWHM. The field of view of each cluster is switched on- and off-source to provide background measurements. The net open area of the seven

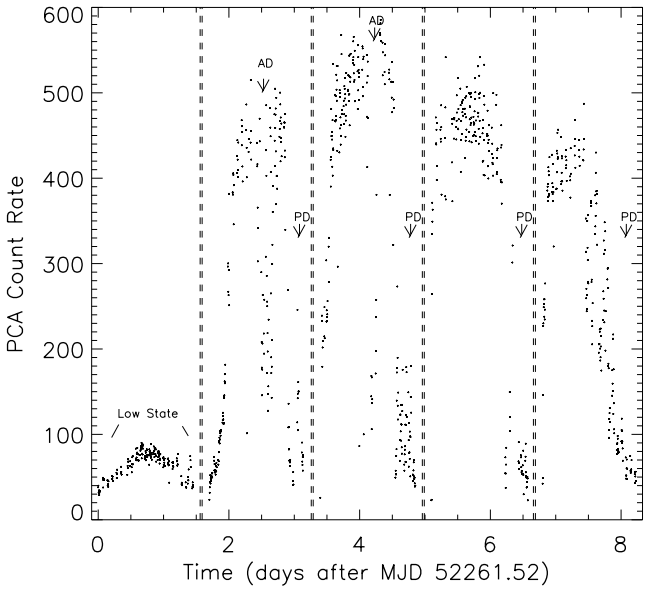


Figure 1. 3–20 keV *RXTE*-PCA light curve of Her X-1. Low state, ADs and PDs are indicated. Vertical dashed lines indicate eclipses of the source.

detectors used for spectroscopy is 1400 cm^2. Each detector covers the energy range of 15–250 keV.

Spectral analysis and error estimation of the spectral parameters are performed using XSPEC. The overall 3–60 keV PCA-HEXTE short high spectrum is extracted. In addition to the overall spectrum, individual PCA spectra are extracted in 3–20 keV.

3 SPECTRAL ANALYSIS

2001 December *RXTE* observation of Her X-1 consists of one low state and four short high state orbits with a total exposure of 281.2 ks. We extract 111 individual PCA spectra in the 3–20 keV energy range to investigate the spectral evolution throughout the whole data set. For the individual PCA spectra, energies lower than 3 keV are ignored due to uncertainties in background modelling while energies higher than 20 keV are ignored as a result of poor counting statistics. Then, the overall 3–60 keV PCA-HEXTE spectrum from the short high state orbits is extracted (Fig. 2). We exclude the 3–60 keV spectrum of the low state orbit since the count rate coming from the channels corresponding to $\gtrsim$ 20 keV is not statistically significant for both PCA and HEXTE. An additional 2 per cent systematic error (see Wilms et al. 1999; Coburn et al. 2000) is added to the statistical errors for both the individual spectra and 3–60 keV PCA-HEXTE spectrum.

It is found that the model consisting of an absorbed power law (Morrison & McCammon 1983) with a high-energy cut-off (White et al. 1983) and an iron line feature modelled as a Gaussian is not able to fit the data well. This is expected since a two-component spectral model with a basic emission spectrum and an absorbed component models or partial covering soft absorption models have been found to fit the main high, short high and low state spectra of Her X-1 (Mihara 1991; Choi et al. 1994a,b; Oosterbroek, Parmar & Martin 1997; Coburn et al. 2000; Oosterbroek et al. 2000; Leahy 2001). We have found that the model containing a partial cold absorber (i.e. the model contains both overall absorption represented by the WABS model and partial absorption represented by the PCFABS in XSPEC) fit the 3–20 keV PCA spectra well for both low state and short high state parts of the observation.

Downloaded from https://academic.oup.com/mnras/article-abstract/361/4/1393/1119646 by MIDDLE EAST TECHNICAL UNIVERSITY LIBRARY user on 23 July 2020

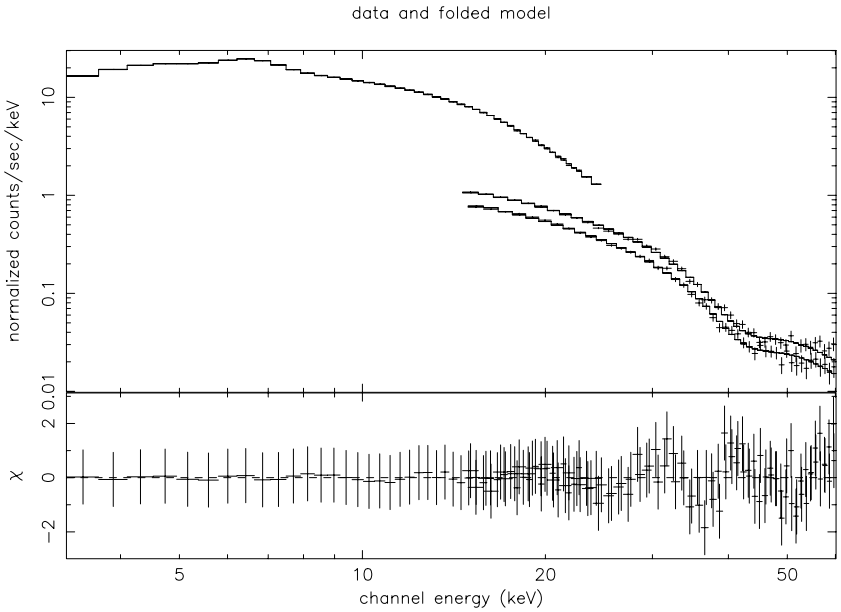


Figure 2. Combined PCA and HEXTE spectrum for the short high state of Her X-1. The bottom panel shows the residuals of the fit in terms of σ values.

Table 1. Sample spectral parameters of individual PCA observations of Her X-1.

Parameter	Low state ($t = 0.34$ d)	Peak of short high ($t = 2.29$ d)	AD ($t = 2.51$ d)	PD ($t = 4.85$ d)
Hydrogen column density (10^{22} cm^{-2})	1.25 ∓ 0.31	1.54 ∓ 0.06	1.80 ∓ 0.34	2.45 ∓ 0.35
Partial covering absorption				
Hydrogen column density (10^{22} cm^{-2})	73.5 ∓ 11.8	34.6 ∓ 4.5	69.2 ∓ 2.8	121.1 ∓ 2.9
Partial cov. frac.	0.46 ∓ 0.07	0.19 ∓ 0.01	0.83 ∓ 0.04	0.81 ∓ 0.04
Iron line energy (keV)	6.72 ∓ 0.04	6.56 ∓ 0.02	6.54 ∓ 0.04	6.81 ∓ 0.03
Iron line sigma (keV)	0.34 ∓ 0.09	0.53 ∓ 0.04	1.13 ∓ 0.05	0.74 ∓ 0.03
Iron normalization ($10^{-3} \times$ cts cm^{-2} s^{-1})	0.62 ∓ 0.10	3.67 ∓ 0.27	6.74 ∓ 0.51	1.41 ∓ 0.11
Power-law normalization ($10^{-2} \times$ cts keV^{-1} cm^{-2} s^{-1})	0.58 ∓ 0.02	5.70 ∓ 0.04	4.11 ∓ 0.06	1.44 ∓ 0.03
3–20 X-ray flux ($10^{-10} \times$ ergs cm^{-2} s^{-1})				
Absorbed	1.02 ∓ 0.07	14.9 ∓ 0.1	5.54 ∓ 0.08	1.60 ∓ 0.03
Unabsorbed	1.37 ∓ 0.09	16.3 ∓ 0.1	9.88 ∓ 0.14	3.37 ∓ 0.07
Reduced χ^2 (33 d.o.f.)	1.45	0.65	0.66	1.35

In Table 1, we present sample results of our spectral fits to the low state, the peak of short high state, AD and PD data. In Fig. 3, we present evolution of spectral parameters during the low and short high state orbits.

To fit the overall 3–60 keV PCA-HEXTE short high state spectrum, we used the same spectral model with an additional cyclotron absorption feature at ∼42 keV (Table 2; Fig. 2). Her X-1 is the first X-ray pulsar to have shown this spectral feature (Truemper et al. 1978). Gruber et al. (2001) showed that the cyclotron resonance energy of Her X-1 changed from ∼34 to ∼42 keV sometime between 1991 and 1993.

4 DISCUSSION AND CONCLUSION

We analysed spectra obtained from continuous *RXTE* monitoring of ∼8.5 d of Her X-1. This rather frequent continuous monitoring, for the first time, enabled the study of the spectral evolution of low state, short high peaks and short high dips within a relatively compact observation period.

For the short high state part, the stability of the power-law index, cut-off energy and e-folding energy throughout the whole monitoring may be an indication of the fact that the accretion geometry and mass accretion rate do not change considerably. This idea is in accordance with the fact that the X-ray flux changes in Her X-1 should primarily be due to the opaque obscuration of the pulsar beam, while there should be no significant variation in the flux emerging initially from the magnetic poles of the pulsar.

We have found some evidence of differences between ADs and PDs in short high state orbits. The first marginal evidence is the higher ratio of unabsorbed flux to absorbed flux for more than ∼50 per cent of PDs compared to ADs (left-hand panel of Fig. 4). For the rest of the PD regions, this ratio is similar to that of the ADs. We

Downloaded from https://academic.oup.com/mnras/article-abstract/361/4/1393/1119646 by MIDDLE EAST TECHNICAL UNIVERSITY LIBRARY user on 23 July 2020

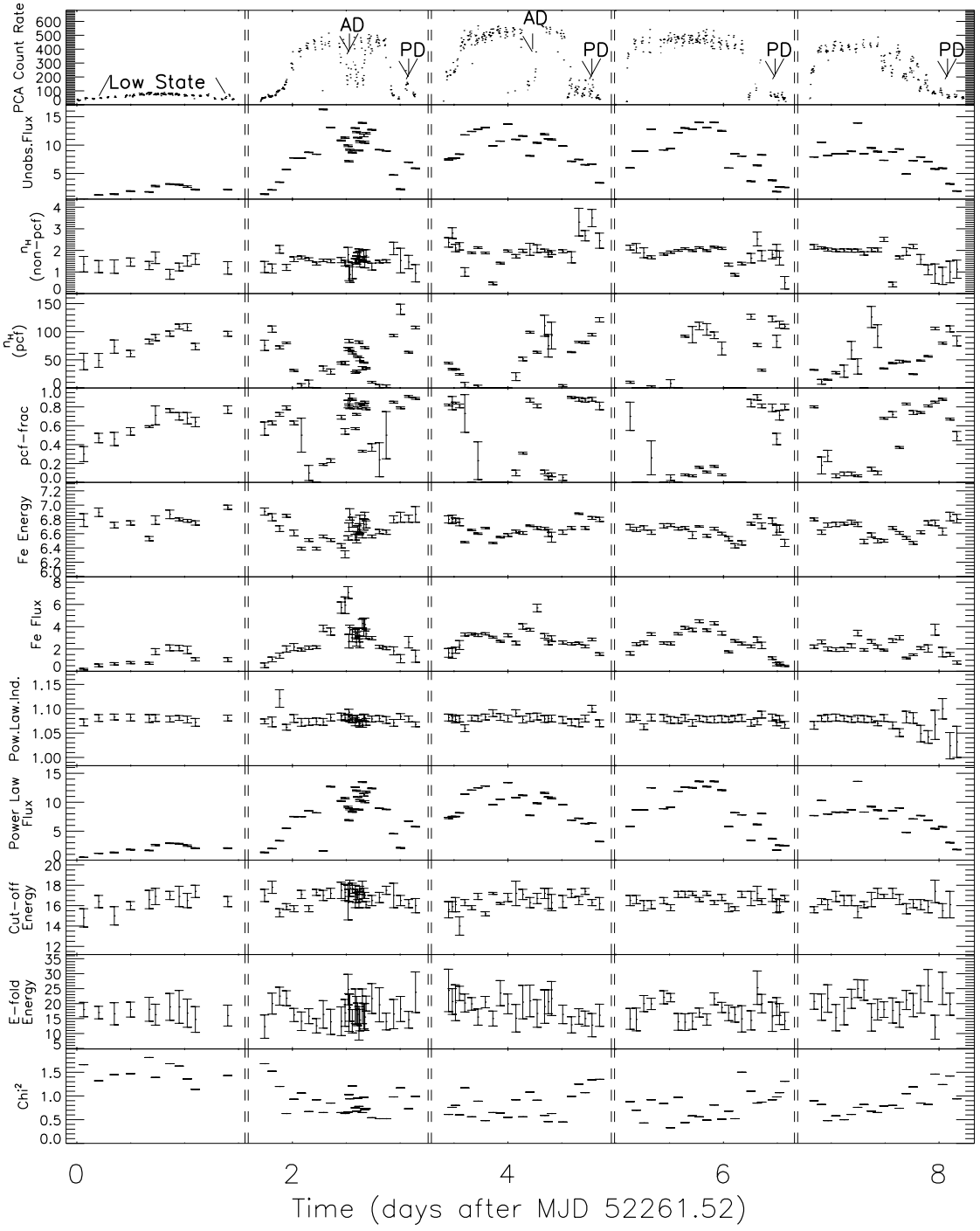


Figure 3. PCA count rate in units of cts s^{-1}, 3–20 keV unabsorbed flux in units of 10^{-10} erg cm^{-2} s^{-1}, overall and partial covering hydrogen column densities in units of 10^{22} cm^2, partial covering fraction, iron line energy in units of keV, iron line flux in units of 10^{-11} erg cm^{-2} s^{-1}, power-law index, 3–20 keV power-law flux in units of 10^{-10} erg cm^{-2} s^{-1}, cut-off and e-folding energies in units of keV and reduced χ^2 as a function of time. Low state, ADs and PDs are indicated. Vertical dashed lines indicate eclipses. Errors indicate 1σ confidence.

consider this ratio as a measure of sum of absorptions coming from the total absorption and partial covering absorption (i.e. greater value of this ratio means more absorption). Then, this marginal evidence shows that absorption is more dominant in PDs compared to ADs. This result is a confirmation of the previous *EXOSAT* (Reynolds & Parmar 1995) and *GINGA* (Leahy 1997) results. From *EXOSAT* observations, it was found that the hydrogen column density was about a few times greater in the PDs compared to that in the ADs, and that partial covering fractions were higher in PDs compared to those in the ADs. Similarly, *GINGA* observations of the absorption dips revealed that n_H was almost an order higher in the PDs compared to that in ADs. This difference of absorption in two types of absorption dips was explained as a sign of the fact that the intersection of the outer rim of the accretion disc with the line of sight is responsible for both types of absorption dips, and different absorptions for both types of dips are only due to the difference in orbital

Downloaded from https://academic.oup.com/mnras/article-abstract/361/4/1393/1119646 by MIDDLE EAST TECHNICAL UNIVERSITY LIBRARY user on 23 July 2020

Table 2. Spectral parameters of PCA-HEXTE observations of the short high state of Her X-1.

Parameter	Value
Hydrogen column density (10^{22} cm^{-2})	2.21 ∓ 0.04
Partial covering absorption	
Hydrogen column density (10^{22} cm^{-2})	65.1 ∓ 0.8
Partial covering fraction	0.32 ∓ 0.02
Gaussian line energy (keV)	6.66 ∓ 0.02
Gaussian line σ (keV)	0.54 ∓ 0.04
Gaussian normalization (cts cm^{-2} s^{-1})	$(2.35 \mp 0.02) \times 10^{-3}$
Power-law photon index	1.09 ∓ 0.03
Cut-off energy (keV)	16.5 ∓ 0.2
e-folding energy (keV)	18.7 ∓ 1.5
Power-law normalization (cts keV^{-1} cm^{-2} s^{-1})	$(3.88 \mp 0.13) \times 10^{-2}$
Cyclotron energy (keV)	42.0 ∓ 0.2
Cyclotron line width (keV)	5.13 ∓ 0.02
Cyclotron line depth	0.99 ∓ 0.02
Calculated X-ray fluxes (3–60 keV in ergs cm^{-2} s^{-1})	
Absorbed	1.22×10^{-9}
Unabsorbed	1.39×10^{-9}
Reduced χ^2	1.07 (127 d.o.f)

phase for these dips (Crosa & Boynton 1980; Leahy 1997). Another piece of evidence supporting this interpretation was the lack of 35-d dependence on the variation of absorption in absorption dips, which is in accordance with the fact that the outer edge of the accretion disc, not being responsible of 35-d cycle, should not be affected by 35-d cycle of precession (Leahy 1997). From the left-hand panel of Fig. 4, we have also found that unabsorbed flux is higher in ADs compared to PDs and that the ratio of unabsorbed flux to absorbed flux decreases with increasing unabsorbed flux independently for both PDs and ADs. Higher unabsorbed flux in ADs is consistent with the general orbital phase dependence of X-ray flux.

On the other hand, the decreasing ratio of unabsorbed flux to absorbed flux (i.e. decreasing absorption) with increasing unabsorbed flux can be explained by the fact that the X-ray flux variation of Her X-1 is the result of opaque obscuration rather than soft absorption (e.g. Still et al. 2001). Variations of unabsorbed flux should be primarily due to the change in opaque obscuration. Opaque obscuration is the result of either obscuration of the accretion disc or the eclipsing stellar companion. This relation, therefore, shows that the regions causing opaque obscuration and soft absorption are not geometrically far away from each other.

Low states in the 35-d cycle of Her X-1 is generally believed to be composed of the phases in which X-rays from the neutron star is obscured (Petterson 1975; Scott & Leahy 1999; Scott et al. 2000; Leahy 2004). The resultant X-ray flux for both normal low states and anomalous low states is a combination of scattered and reflected components and has been found to fit well, except for normalizations and excess absorption, to high state spectrum models (e.g. Coburn et al. 2000). Coburn et al. (2000) also found that absorption can be modelled with a cold partial absorber with $n_{\rm H} \sim 5 \times 10^{23}$ cm^{-2} and partial covering fraction of $\sim$0.7 for both normal and anomalous low states. Results of our low state fits, giving values $\sim(5\text{–}10) \times 10^{23}$ cm^{-2} and $\sim$0.3–0.8 for $n_{\rm H}$ and the partial covering fraction, respectively, are in agreement with those results.

From the right-hand panel of Fig. 4, the iron line flux is correlated, in general, with the X-ray flux for both short high state and low state observations. However, there is marginal evidence of higher iron line flux for the ADs. An increase in the strength of the iron line feature in the ADs is a natural consequence of the fact that we have some of the X-ray flux coming from the neutron star and passing through the outer rim of the accretion disc, which is possibly enhancing this iron line feature, so the resultant iron line flux increases in the ADs. Although the origin of the ADs and PDs is similar, the iron line flux is not significantly higher for the PDs. This may be related to an orbital phase difference between ADs and PDs. Future observations of PDs of Her X-1 will be useful to study the variation of the iron line feature.

The peak energy of the iron line feature is, in general, at $\sim$6.6 keV for the short high state. From Fig. 3, the peak energy tends to increase at the initial short high turn-on (around $\sim$1.9 d) AD of the first short high orbit and PDs. The iron line feature is also found to peak at higher energies ($\sim$6.8 keV) in the low state. Iron line energy peaking at higher energies is a sign of the fact that this feature does not consist of only the Kα Fe emission line. In fact, it has recently been noted that the Kα Fe line emission tends to be less powerful in short high and low states compared to the main high state (Zane et al. 2004). Zane et al. (2004), using *XMM–Newton* observations, has also been able to resolve a secondary iron line feature (Fe XXVI) peaking at

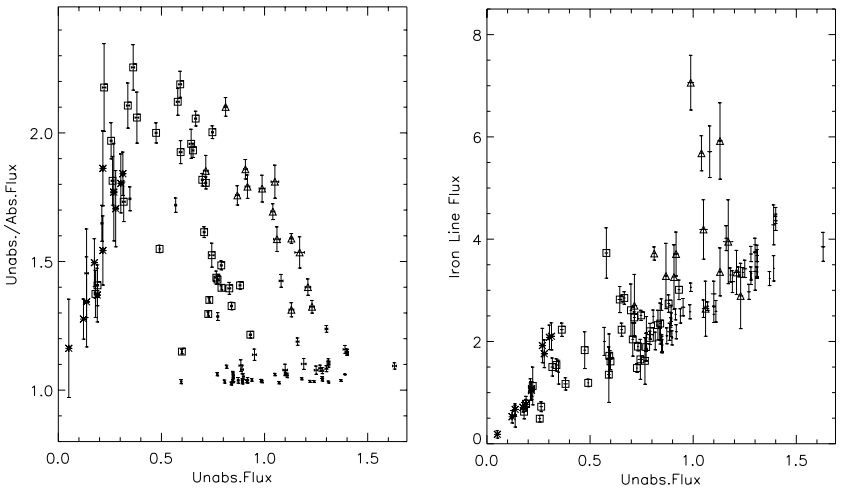


Figure 4. Variation of the ratio of the 3–20 keV unabsorbed flux to the 3–20 keV absorbed flux (left), and variation of iron line flux in units of 10^{-11} erg cm^{-2} s^{-1} (right) as a function of 3–20 keV unabsorbed flux in units of 10^{-10} erg cm^{-2} s^{-1}. Asterisks, triangles and squares denote low state, AD and PD, respectively.

Downloaded from https://academic.oup.com/mnras/article-abstract/361/4/1393/1119646 by MIDDLE EAST TECHNICAL UNIVERSITY LIBRARY user on 23 July 2020

~6.9–7.0 keV, which is present only in the low state and the short high state. The spectral resolution of *RXTE*-PCA is not good enough to resolve these lines but the higher peak energies of the resultant iron line feature may be a clue of the presence of iron line components other than the Kα emission line.

ACKNOWLEDGMENTS

We acknowledge D. M. Scott for his guidance and we thank him for the useful discussions. S.C.İ. acknowledges the Integrated Doctorate Programme scholarship from the Scientific and Technical Research Council of Turkey (TÜBİTAK).

REFERENCES

Baykal A. et al., 1993, MNRAS, 265, 347
Boyd P., Still M., Corbet R., 2004, ATEL, 307
Choi C. S., Nagase F., Makino F., Dotani T., Min K. W., 1994a, ApJ, 422, 799
Choi C. S., Nagase F., Makino F., Dotani T., Kitamoto S., Takahama S., 1994b, ApJ, 437, 449
Coburn W. et al., 2000, ApJ, 543, 351
Coburn W., Heindl W. A., Rothschild R. E., Gruber D. E., Kreykenbohm I., Wilms J., Kretschmar P., 2002, ApJ, 580, 394
Crosa L., Boynton P. E., 1980, ApJ, 235, 999
Dal Fiume D., Orlandini M., Casumano G., 1998, A&A, 329, L41
Davidsen A., Patrick H. J., Middleditch J., Smith H. E., 1972, ApJ, 177, L97
Deeter J., Crosa L., Gerend D., Boynton P. E., 1976, ApJ, 206, 861
Endo T., Nagase F., Mihara T., 2000, PASJ, 52, 223
Gerend D., Boynton P. E., 1976, ApJ, 209, 562
Giacconi R., Gursky H., Kellogg E., Levinson R., Schreier E., Tannanbaum H., 1973, ApJ, 184, 227
Gruber D. E., Heindl W. A., Rothschild R., Coburn W., Staubert R., Kreykenbohm I., Wilms J., 2001, ApJ, 562, 499
Jahoda K., Swank J. H., Giles A. B., Stark M. J., Strohmayer T., Zhang W., Morgan E. H., 1996, Proc. SPIE, 2808, 59
Leahy D. A., 1995, A&ASS, 113, 21
Leahy D. A., 1997, MNRAS, 287, 622
Leahy D. A., 2001, ApJ, 547, 449
Leahy D. A., 2004, AN, 325, 205
Leahy D. A., Yoshida A., Matsuoka M., 1994, ApJ, 434, 341
Middleditch J., 1983, ApJ, 275, 278
Mihara T., Okashi T., Makishima K., Nagase F., Kitamoto S., Koyama K., 1991, PASJ, 43, 501
Morrison R., McCammon D., 1983, ApJ, 270, 119
Ogelman H. 1987, A&A, 172, 79
Oosterbroek T., Parmar A. N., Martin D. D. E., 1997, A&A, 327, 215
Oosterbroek T., Parmar A. N., Dal Fiume D., Orlandini M., Santangelo A., Del Sordo S., Segreto A., 2000, A&A, 353, 575
Parmar A. N., Pietsch W., McKechnie S., White N. E., Truemper J., Voges W., Barr P., 1985, Nat, 313, 119
Petterson J. A., 1975, ApJ, 201, L61
Ramsay G., Zane S., Jimenez-Garate M. A., 2002, astro-ph/0201526
Reynolds A. P., Parmar A. N., 1995, A&A, 297, 747
Rothschild R. E. et al., 1998, ApJ, 496, 538
Shakura N. I., Ketsaris N. A., Prokhorov M. E., Postnov K. A., 1998, MNRAS, 300, 992
Scott D. M., Leahy D. A., 1999, ApJ, 510, 974
Scott D. M., Leahy D. A., Wilson R. B., 2000, ApJ, 539, 392
Stelzer B., Wilms J., Staubert R., Gruber D., Rothschild R., 1999, A&A, 342, 736
Still M., O'Brien K., Horne K., Hudson D., Boroson B., Vrtilek S. D., Quantrell H., Fiedler H., 2001, ApJ, 553, 776
Tananbaum H., Gursky H., Kellogg E. M., Levinson R., Schreier E., Giacconi R., 1972, ApJ, 174, L143
Truemper J., Pietsch W., Reppin C., Voges W., Staubert R., Kendziorra E., 1978, ApJ, 219, L105
Ushimaru N., Tawara Y., Koyama K., 1989, PASJ, 41, 441
Vrtilek S. D. et al., 1994, ApJ, L436, 9
White N. E., Swank Swank J. H., Holt S. S., 1983, ApJ, 270, 711
Wilms J., Nowak M. A., Dove J. B., Fender R. P., di Matteo T., 1999, ApJ, 522, 460
Zane S., Ramsay G., Jimerez-Garate M. A., den Harder J. W., Hailey C. J., 2004, MNRAS, 350, 506

This paper has been typeset from a TEX/LATEX file prepared by the author.

Downloaded from https://academic.oup.com/mnras/article-abstract/361/4/1393/1119646 by MIDDLE EAST TECHNICAL UNIVERSITY LIBRARY user on 23 July 2020